Int. J. Heat Mass Transfer. Vol. 33, No. 5, pp. 1003–1012, 1990
Printed in Great Britain

0017–9310/90 $3.00 + 0.00

Unsteady vaporization of fuel droplets in a convective environment with varying ambient conditions

R. P. GAKKHAR and S. PRAKASH
Department of Mechanical and Industrial Engineering, University of Roorkee, Roorkee 247667, India

(*Received* 28 *October* 1986 *and in final form* 12 *October* 1988)

Abstract—In the present work, a comparison of an integral and the two-dimensional boundary layer solution for the unsteady droplet vaporization problem has been made. The quasi-steady two-dimensional conservation equations (uncoupled from the liquid-phase) for the axisymmetric gas-phase boundary layer have been solved for both the circulating and the non-circulating droplets. The integral approach developed earlier (S. Prakash and W. A. Sirignano, *Int. J. Heat Mass Transfer* **23**, 253–268 (1980)) for the gas-phase analysis of the droplet vaporization problem has been modified and extended for time-dependent ambient conditions, namely temperature, pressure, fuel mass fraction and free stream velocity. The effect of variation of these ambient parameters on the droplet vaporization has also been studied. It is found that the integral approach is reasonably good in predicting the heat and mass fluxes as well as the velocity temperature and the fuel mass fraction profiles across the boundary layer. Also the droplet lifetime is predicted reasonably well by the integral approach. The difference of fuel mass fraction at the droplet surface and in the ambience, $(Y_{F_s} - Y_{F_\infty})$, through its effect on droplet surface temperatures affects the droplet lifetime, though not significantly. Also, the rate of droplet heating during the earlier part of the droplet lifetime has a significant effect on the vaporization rate and the droplet lifetime. The lower values of ambient pressure during the earlier part of the droplet lifetime result in higher vaporization rates. As expected, the mass vaporization rates are reduced and the droplet lifetime is increased because of drag.

INTRODUCTION

THE IMPORTANCE of the study of vaporization and combustion of liquid fuel droplets is well known [1]. Generally, as in spray combustion, the droplets vaporize and burn in a strong convective flow field with varying ambient conditions. The relative velocity between the droplet and the hot ambient gases decreases due to drag. Moreover, a droplet may encounter conditions of varying ambient temperature and fuel mass fraction as it approaches a hot flame zone. These varying ambient conditions, along with the unsteady heating and shrinking of the droplet, make the problem of droplet vaporization in a spray essentially unsteady. The semi-empirical correlations which are generally used to predict mass vaporization rate under quasi-steady conditions are, therefore, not adequate for use in the overall modelling of spray processes.

Prakash and Sirignano [2] have studied unsteady convective droplet vaporization, with liquid-phase circulation, for constant ambient conditions. They developed the gas-phase analysis based on the integral approach. However, the accuracy of the integral approach, which requires that certain arbitrary conditions at the interface be satisfied, has not been determined. In the present work a comparison of an integral and the two-dimensional boundary layer solutions for the unsteady droplet vaporization problem has been made. The gas-phase analysis using the integral approach developed by Prakash and Sirignano [2] for constant ambient conditions has been modified and extended to take into account the time-dependent ambient conditions. The coupled problem comprising the gas-phase analysis coupled to the one-dimensional unsteady liquid-phase heating without liquid-phase motion has been solved for temporally varying ambient conditions. The present study, it is hoped, will provide better understanding of the coupling between the vaporization rate and the varying ambient gas-phase conditions.

FORMULATION

The characteristic time for changes in the gas-phase boundary layer is the residence time [$O(10\ \mu s)$] in the neighbourhood of the droplet and is very much smaller than the droplet life time [$O(5$ ms$)$] for a droplet of the size usually encountered in many practical situations. However, the changes in the ambient conditions considered here take place on a time scale which is of the same order as the droplet lifetime. Therefore, the quasi-steady gas-phase assumption can be employed.

With the usual assumptions of unity Schmidt and Prandtl numbers in the gas-phase, equal and constant binary diffusion coefficients and constant specific heats at constant pressure for various components, the absence of Soret, Dufour and radiation effects and

NOMENCLATURE

c_0–c_4	coefficients of fuel mass fraction profile
D	diffusion coefficient
f'	velocity ratio, u/u_e
g	enthalpy ratio, h/h_e
L	latent heat of vaporization of fuel
L'	modified latent heat of vaporization, defined in equation (9)
$\dot{m}''_{sn}$	non-dimensional local vaporization mass flux, $[(\rho v)_s/\rho_\infty U_\infty]\cdot\sqrt{(Re_g)}$
$\overline{\dot{m}''_{sn}}$	average non-dimensional mass vaporization rate, $(\overline{\dot{m}''_s}/\rho_\infty U_\infty\sqrt{(Re_g)})$
M_i	molecular weight of ith species
p	pressure
$\dot{q}''_{gn}$	non-dimensional gas-side heat flux, $(\dot{q}''_g/\rho_\infty U_\infty h_\infty)\sqrt{(Re_g)}$
$\overline{\dot{q}''_{gn}}$	average non-dimensional gas-side heat flux
$\dot{q}''_{ln}$	non-dimensional liquid-side heat flux, $(\dot{q}''_l/\rho_\infty U_\infty h_\infty)\sqrt{(Re_g)}$
$\overline{\dot{q}''_{ln}}$	average non-dimensional liquid-side heat flux
r_s	normal distance of the interface from the axis of symmetry
r_{sn}	r_s/R
R	droplet radius, universal gas constant
Re	Reynolds number
$\bar{s}^*$	transformed x-coordinate
$\bar{s}$	non-dimensional transformed x-coordinate
T	temperature
u	gas-phase velocity in the x-direction
u_{en}	u_e/U_∞
U_∞	free stream velocity relative to the droplet
v	gas-phase velocity in the y-direction
V_n	non-dimensional gas-phase velocity in the y-direction
V	normal velocity parameter, defined in equation (15)
w_i	rate of production of ith species
x	gas-phase tangential coordinate
y	gas-phase boundary layer coordinate normal to the interface
Y_F	fuel mass fraction
Y_i	mass fraction of ith species
z	mass fraction ratio, defined in equation (10).

Greek symbols

α	thermal diffusivity
β	pressure gradient parameter
δ_{Y_F}	boundary layer species thickness defined in equation (22)
η	transformed boundary layer coordinate normal to the interface
θ	tangential coordinate direction
λ	thermal conductivity
μ	density
ρ	density
$(\rho\mu)_{en}$	$(\rho\mu)_e/\rho_\infty\mu_\infty$
τ	non-dimensional time, $\alpha_l t/R_0^2$.

Subscripts

e	edge of the boundary
F	fuel
g	gas-phase
l	liquid-phase
n	non-dimensional quantity
s	gas–liquid interface
∞	free stream values.

low Mach number flow, the conservation equations for the quasi-steady axisymmetric boundary layer, in orthogonal boundary layer coordinates, for compressible flow over a sphere can be written, neglecting the effect of curvature, as follows:

$$\frac{\partial}{\partial x}(\rho u r_s)+\frac{\partial}{\partial y}(\rho v r_s)=0 \tag{1}$$

$$\rho\left(u\frac{\partial u}{\partial x}+v\frac{\partial u}{\partial y}\right)=-\frac{\partial p}{\partial x}+\frac{\partial}{\partial y}\left(\mu\frac{\partial u}{\partial y}\right) \tag{2}$$

$$\rho\left(u\frac{\partial h}{\partial x}+v\frac{\partial h}{\partial y}\right)-u\frac{\partial p}{\partial x}=\frac{\partial}{\partial y}\left(\lambda\frac{\partial T}{\partial y}\right)+\frac{\partial}{\partial y}\left[\rho\sum_{i=1}^{N}D_i\frac{\partial Y_i}{\partial y}h_i\right]+\mu\left(\frac{\partial u}{\partial y}\right)^2 \tag{3}$$

$$\rho\left(u\frac{\partial Y_i}{\partial x}+v\frac{\partial Y_i}{\partial y}\right)=\frac{\partial}{\partial y}\left(\rho D\frac{\partial Y_i}{\partial y}\right)+w_i \tag{4}$$

and the equation of state is

$$p=\sum_{i=1}^{N}\frac{Y_i}{M_i}\rho RT. \tag{5}$$

The boundary conditions are:

(i) at the edge of the boundary layer

$$u=u_e(x,t)$$
$$Y_F=Y_{Fe}(t)$$
$$T=T_e(t); \tag{6}$$

(ii) at the surface of the droplet

$$\frac{u}{u_e}=\frac{u_s}{u_e}$$
$$Y_F=Y_{Fs}(t)$$
$$T=T_s(t). \tag{7}$$

The conservation of fuel mass flux and heat flux at the interface is expressed as

$$\left[\rho D \frac{\partial Y_F}{\partial y}\right]_s = (\rho v)_s (Y_{Fs} - 1) \tag{8}$$

and

$$\left[\frac{\lambda}{C_p}\frac{\partial h}{\partial y}\right]_{s,g} = (\rho v)_s L + \left(\lambda \frac{\partial T}{\partial y}\right)_{s,l} = (\rho v)_s L'. \tag{9}$$

The velocity at the edge of the boundary layer u_e is a function of both x and t. It varies with time on account of the variation of relative free stream velocity, U_∞, due to drag.

In the present analysis the velocity distribution outside the boundary layer is assumed to be potential flow over a sphere. However, for a better description of the flow field for Reynolds numbers of the order of 100, the actual velocity distribution for viscous flow should be considered. The ambient temperature, pressure and the fuel mass fraction are assumed to be known functions of time.

The surface temperature $T_s(t)$ is known from the liquid-phase analysis and $Y_{Fs}(t)$ is related to $T_s(t)$ through a phase equilibrium relationship. In the present analysis, the liquid-phase heating has been approximated as one-dimensional, in the absence of liquid-phase motion, for simplicity. It has been shown by Prakash and Krishan [3] that in the absence of liquid-phase motion, the difference in the averaged heat flux, mass flux, and the surface and the centre temperature due to one-dimensional approximation is less than 5%. The error in the droplet lifetime is even less.

Two-dimensional approach

The boundary layer equations (1)–(4) are transformed into similarity form by the change of variables that combine the Levy–Mangler and Howarth–Dorodintzyn transformations.

Defining

$$\bar{s}^*(x) = \int_0^x \rho_e \mu_e u_e r_s^2 \, dx$$

and

$$\eta(x, y) = \frac{\rho_e u_e r_s}{(2\bar{s})^{1/2}} \int_0^y \frac{\rho}{\rho_e} \, dy \tag{10}$$

as the independent variables and

$$f' = u/u_e, \quad g = h/h_e, \quad z_i = \frac{Y_i}{1 - Y_{ie}}$$

as the dependent variables, the boundary layer equations in the non-dimensional form become:

$$2\bar{s}\frac{\partial f'}{\partial \bar{s}} + \frac{\partial f}{\partial \eta} + \frac{\partial v}{\partial \eta} = 0 \tag{11}$$

$$2\bar{s}f'\frac{\partial f'}{\partial \bar{s}} + V\frac{\partial f'}{\partial \eta} = \frac{\partial^2 f'}{\partial \eta^2} + \beta\left[\frac{\rho_e}{\rho} - (f')^2\right] \tag{12}$$

$$2\bar{s}f'\frac{\partial g}{\partial \bar{s}} + V\frac{\partial g}{\partial \eta} = \frac{\partial^2 g}{\partial \eta^2} \tag{13}$$

$$2\bar{s}f'\frac{\partial z_i}{\partial \bar{s}} + V\frac{\partial z_i}{\partial \eta} = \frac{\partial^2 z_i}{\partial \eta^2} \tag{14}$$

where

$$\bar{s}(x) = \frac{\bar{s}^*}{\rho_\infty u_\infty \mu_\infty R^3}$$

$$V = \frac{2\bar{s}}{(\rho\mu)_{en} u_{en} r_{sn}^2}\left[\frac{\partial f}{\partial \eta}\frac{\partial \eta}{\partial x_n} + \frac{(\rho v)_n r_{sn}}{\sqrt{(2\bar{s})}}\right]$$

and

$$\beta = \frac{2\bar{s}}{u_e}\frac{du_e}{d\bar{s}}. \tag{15}$$

The boundary conditions become:

(i) at the surface of the droplet, i.e.

$$f'(0) = \frac{u_s}{u_e}, \quad g(0) = \frac{h_s}{h_e}, \quad z(0) = \frac{Y_{Fs}}{1 - Y_{Fe}}; \tag{16}$$

(ii) at the edge of the boundary layer, i.e. $\eta \to \infty$

$$f'(\infty) = 1, \quad g(\infty) = 1, \quad z(\infty) = \frac{Y_{Fe}}{1 - Y_{Fe}}. \tag{17}$$

The conservation of fuel mass flux and heat flux at the interface requires

$$V|_{\eta=0} = \left[\frac{1 - Y_{Fe}}{z(0)(1 - Y_{Fe}) - 1}\right]\left.\frac{\partial z_i}{\partial \eta}\right|_{\eta=0} \tag{18}$$

and

$$V|_{\eta=0} = \frac{1}{L'}\left.\frac{\partial g}{\partial \eta}\right|_{\eta=0}. \tag{19}$$

Equations (11)–(14), along with the boundary conditions (16) and (17) and the conservation conditions at the interface, namely equations (18) and (19), are solved by a predictor–corrector technique suggested by Douglas and Jones [4].

Integral approach

The system of equations (1)–(4) and the boundary conditions (6) and (7) were solved using an integral approach as described by Prakash and Sirignano [2]. Since the method of solution and the equations closely resemble those in ref. [2], only the major differences are given here. Also, the same nomenclature as in ref. [2] has been adopted here.

Equations (2) and (3), when integrated across the boundary layer thickness 'δ', become

$$\frac{d\delta_2}{dx} + \frac{u_e'}{u_e}\left(2 + \frac{\delta_1}{\delta_2} + \frac{r_s' u_e}{r_s u_e'}\right)\delta_2 - \frac{(\rho v)_s}{\rho_e u_e}\left(1 - \frac{u_s}{u_e}\right) = \left(\frac{\left(\mu \frac{\partial u}{\partial y}\right)_s}{\rho_e u_e^2}\right) \tag{20}$$

$$\frac{d\delta_H}{dx} + \frac{u_e'}{u_e}\left(1 + \frac{r_s'}{r_s}\frac{u_e}{u_e'}\right)\delta_H - \frac{(\rho v)_s}{\rho_e u_e}\left(1 - \frac{h_s}{h_e}\right) = \left(\frac{\left(\mu \frac{\partial h}{\partial y}\right)_s}{\rho_e u_e h_e}\right). \quad (21)$$

To include the situation of the non-zero fuel mass fraction in the free stream (Y_{Fe}), δ_{Y_F} is defined as given below

$$\delta_{Y_F} = \int_0^{\delta} \frac{\rho u}{\rho_e u_e}(Y_F - Y_{Fe})\,dy \quad (22)$$

and correspondingly equation (4) becomes

$$\frac{d\delta_{Y_F}}{dx} + \frac{u_e'}{u_e}\left(1 + \frac{r_s'}{r_s}\frac{u_e}{u_e'}\right)\delta_{Y_F} - \frac{(\rho v)_s}{\rho_e u_e}(Y_{Fs} - Y_{Fe}) = \frac{\left(\mu \frac{\partial Y_F}{\partial y}\right)_s}{\rho_e u_e}. \quad (23)$$

It should be noted that in the present analysis, the ambient conditions, and correspondingly u_e, ρ_e, h_e and Y_{Fe} are time-dependent.

Polynomial profiles of the fourth degree in the transformed variable are assumed for velocity, density and fuel mass fraction. Let

$$\frac{u}{u_e} = \sum_{n=0}^{4} a_n \eta^n; \quad \frac{\rho}{\rho_e} = \sum_{n=0}^{4} b_n \eta^n; \quad \frac{Y_{Fe}}{1 - Y_{Fe}} = \sum_{n=0}^{4} c_n \eta^n$$

where a_n, b_n, c_n are functions of x and time. The polynomial profile for fuel mass fraction takes into account the ambient fuel mass fraction Y_{Fe}.

The integrated momentum, energy and fuel conservation equations (20), (21) and (23) are non-dimensionalized and after substantial algebraic manipulation are expressed as coupled non-linear ordinary differential equations. These ordinary differential equations are solved numerically as described in ref. [2] for δ', b_1 and m_s''. Once these quantities are known, other relevant quantities are calculated.

RESULTS, DISCUSSION AND CONCLUSIONS

Comparison of the integral and the two-dimensional analysis

In the integral approach, the boundary layer equations are integrated across the thickness of the boundary layer. The resulting non-linear ordinary differential equations, along with the selected interface and the boundary conditions, are solved. For the solution of these coupled ordinary differential equations, fourth degree polynomial profiles for velocity, temperature and fuel mass fraction are assumed. The solution provides the heat and mass fluxes at the interface. The various coefficients associated with the polynomials and consequently the velocity, temperature and the fuel mass fraction profile across the boundary layer can also be determined from the solution.

In the two-dimensional analysis, the boundary layer equations, along with the appropriate boundary conditions, are solved to get the velocity, temperature and fuel mass fraction profiles. From these profiles the mass and heat fluxes are then calculated.

In the vaporization problem, the mass and heat fluxes at the interface are of interest. However, these fluxes are related to the gradients of the profiles at the droplet surface. It would, therefore, be appropriate to compare the detailed profiles, in addition to the comparison of heat and mass fluxes.

For the purpose of comparison, the gas-phase equations, uncoupled from the liquid-phase, are solved for n-decane droplets vaporizing in air at 1000 K and at 10 atm pressure. Both the circulating and the non-circulating situations have been considered. For the circulating situation, a constant value of $u_s/u_e = 0.1$ has been assumed, while for the non-circulating case u_s/u_e is zero. Because the maximum differences in the local mass and heat fluxes computed by the two approaches are expected to occur when the vaporization rate is high, a relatively high value of the surface temperature of 498.47 K was taken, which would be the temperature attained by a n-decane droplet towards the end of its lifetime. Velocity, temperature and fuel mass fraction profiles are computed at different locations along the droplet surface.

The non-dimensional coordinate, normal to the droplet surface (η), has been defined differently in the two approaches. However, the coordinate η, defined by equation (10) for the two-dimensional approach, was used for the purpose of comparison.

Figures 1 and 2 show the velocity, temperature and fuel mass fraction profiles computed by the two approaches at $\theta = 0$ and 1.8 rad, respectively, along the droplet surface, for the circulating and non-circulating droplets. The profiles coincide at the surface of the droplet and at the edge of the boundary layer, because of the imposed boundary conditions. It should be noted that the difference in the profiles obtained by the two approaches is quite small. Near the point of zero shear stress, i.e. at $\theta = 180$ rad (Fig. 2), it should be noted that the differences in the profiles for the non-circulating droplet are greater than for the circulating droplet. It appears that the integral approach is good for the circulating droplet, even near the point of zero shear stress, when compared to the non-circulating droplet. This is because the point of zero shear stress for the non-circulating droplet is also the separation point, while for the circulating droplet separation occurs further downstream of the zero shear stress point and is closer to the rear stagnation point.

The gradients of the fuel mass fraction and temperature profiles at the droplet surface are proportional to the mass and heat fluxes respectively. Figure 3 shows the variation of heat and mass fluxes with angular position using the two approaches. It

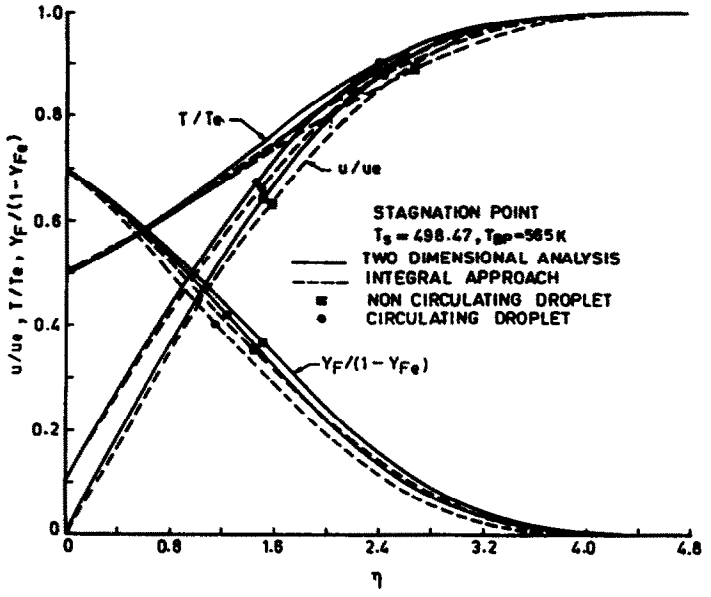

FIG. 1. Velocity, temperature and fuel mass fraction profiles at the stagnation point.

can be observed that the difference using the two approaches is of the order of 10% (higher with the integral approach) except in a small region near the point of zero shear stress. However, the contribution of this region, near the point of zero shear stress, towards the overall heat and mass transfer is quite small. Therefore, the integral approach can be used as a good approximation to predict heat and mass fluxes for a vaporizing droplet.

To compare the droplet lifetime estimated by the two approaches, the coupled problem was solved for the non-circulating, n-decane droplet vaporizing in air at 1000 K and 10 atm pressure. The gas-phase boundary layer analysis was coupled to one-dimensional unsteady liquid-phase heating [3]. However, for the purpose of comparison, the contribution of the wake region towards the average mass vaporization rate and towards the gas- and the liquid-side heat fluxes was not considered because the boundary layer solution is not valid in this region, though its contribution is of the order of 15%, for Reynolds numbers of the order of 100 [5].

Figure 4 shows the temporal variation of the average mass vaporization rate, $(R/R_0)^{3/2}$, the gas- and liquid-side heat fluxes and the droplet surface temperature obtained by the two approaches for the

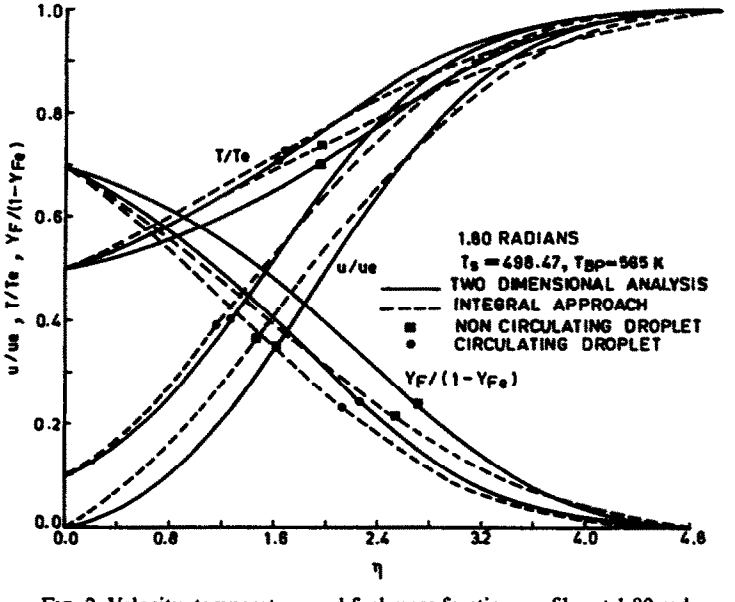

FIG. 2. Velocity, temperature and fuel mass fraction profiles at 1.80 rad.

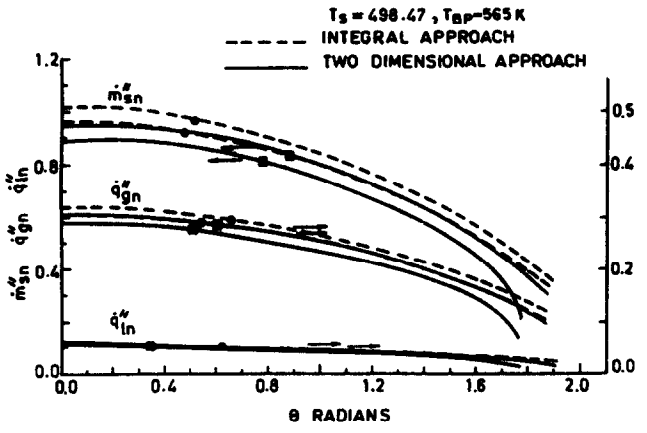

FIG. 3. Vaporization mass flux, gas- and liquid-side heat flux variations with θ.

coupled problem. It is observed that the integral approach overestimates the mass vaporization rate as compared to the two-dimensional analysis, throughout the droplet lifetime. This is because the gas-side heat flux predicted by the integral approach is higher, whereas the liquid-side heat flux is almost the same (Fig. 4), leading to higher values of surface temperature throughout the droplet lifetime. Consequently the droplet lifetime is underestimated by about 12% using the integral approach.

It can be observed from the above comparison that the solution obtained by using the integral approach for the gas-phase boundary layer is reasonably good, particularly when it is noted that the other approximations used in the droplet vaporization problem involve larger errors. Further, the computation time required with the integral approach was about half of that required with the two-dimensional approach. However, it may be pointed out that the effort required to set the problem using the integral approach is greater. Because of a limitation on computer time, the integral approach was, therefore, used to solve the coupled problem with the time varying ambient conditions. The coupled problem was solved for three fuels, namely n-hexane, n-decane and n-hexadecane, which have a wide range of volatility.

Effect of varying ambient conditions

The time varying ambient parameters considered in the present study are pressure, temperature, fuel mass fraction and free stream velocity. The assumed temporal variations of pressure, temperature and fuel mass fraction are shown in Fig. 5. Two cases of ambient pressure variation have been considered. In the first case, the pressure varies linearly with time from 5 to 15 atm for n-decane and n-hexane and from 4 to

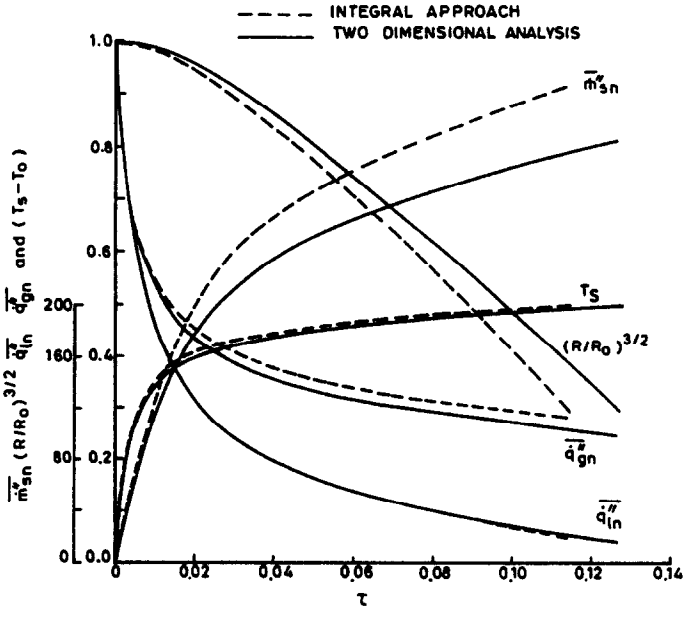

FIG. 4. Comparison of results by two approaches.

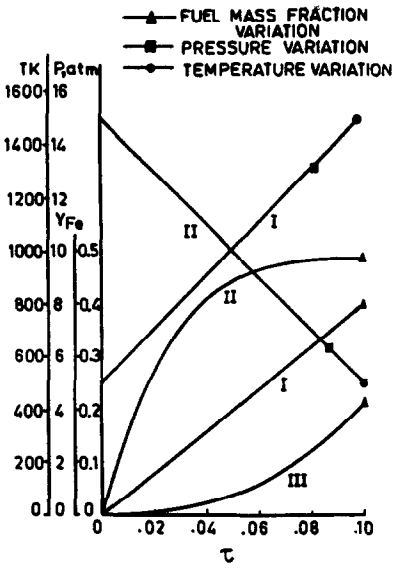

FIG. 5. Ambient temperature, pressure and fuel mass fraction variations considered.

12 atm for n-hexadecane, since the critical pressure for n-hexadecane is 14 atm. This situation is similar to that in a diesel engine, where fuel injection and vaporization of fuel droplets take place towards the end of the compression stroke, when the pressure within the cylinder is rising. In the second case, the pressure varies linearly from 15 to 5 atm for n-decane and n-hexane and from 12 to 4 atm for n-hexadecane droplets. This situation is similar to the situation of late injection in the diesel engine.

Two cases of ambient temperature variation with time have been considered. In the first case the ambient temperature increases linearly from 500 to 1500 K. This represents the situation in which the droplet is approaching a hotter region. In the second case, the ambient temperature decreases linearly from 1500 to 500 K. This represents a situation in which the droplet is moving away from the hotter zone.

Three cases of ambient fuel mass fraction variation with time have been considered (Fig. 5). In all these cases, Y_{Fe} remains well below the fuel mass fraction at the droplet surface, Y_{Fs}, throughout the droplet lifetime. All these cases represent the practical situations in which a fuel droplet is moving in a region of heterogeneous fuel–air mixture, similar to the situation in a diesel engine.

The variation in the relative free stream velocity has been considered by taking into account the drag forces acting on the droplet. The drag coefficient variation with Reynolds number for vaporizing droplets was computed, as suggested by Yuen and Chen [6], using a standard drag curve and modifying the Reynolds number. For calculating the Reynolds number, the free stream density was used, while the viscosity was evaluated at the reference temperature T_r and the reference fuel mass fraction $Y_{F,r}$ which are defined below

$$T_r = T_s + (T_\infty - T_s)/3$$

and

$$Y_{F,r} = Y_{Fs} + (Y_{Fe} - Y_{Fs})/3.$$

The drag coefficient–Reynolds number correlations for a solid sphere were taken from Morsi and Alexander [7].

The results obtained with varying ambient parameters are discussed below.

It is observed from Fig. 6 that for all the three cases of ambient fuel mass fraction variation considered, the mass vaporization rates are lower, the gas-side heat fluxes are hardly affected, while the liquid-side heat fluxes and droplet surface temperatures are higher, when fuel vapours are present in the ambience.

Figure 7 shows the temporal variation of $(Y_{Fs} - Y_{Fe})$, the difference of fuel mass fraction at the droplet surface and in the ambience, for the three cases considered. An observation of the variation of mass vaporization rate (Fig. 6) shows that it follows the variation of $(Y_{Fs} - Y_{Fe})$ because it is the motive force for the diffusion of fuel. However, the gas-side heat flux is not affected much due to the small modifications of the thermal boundary layer. Consequently, the liquid-side heat flux and the droplet surface temperatures are higher when fuel is present in the ambience. It should be noted that the percentage reduction in the mass vaporization rate is much smaller when compared with the reductions in $(Y_{Fs} - Y_{Fe})$ for the three situations considered, because the vaporization rate is primarily controlled by the heat flux received from the ambience for the

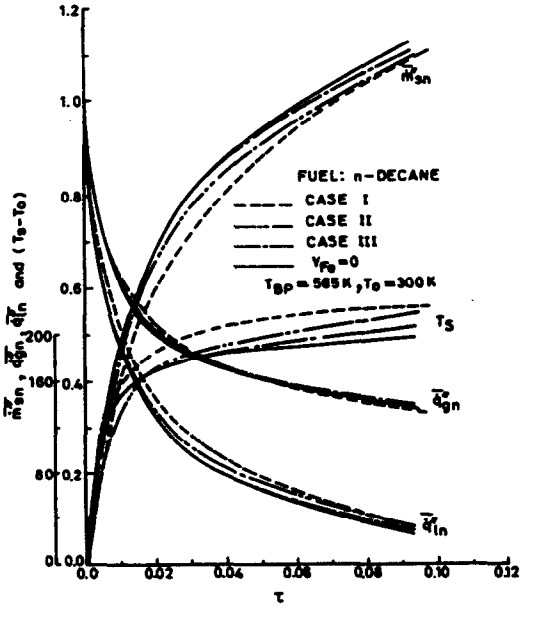

FIG. 6. Effect of temporal variation of ambient fuel mass fraction.

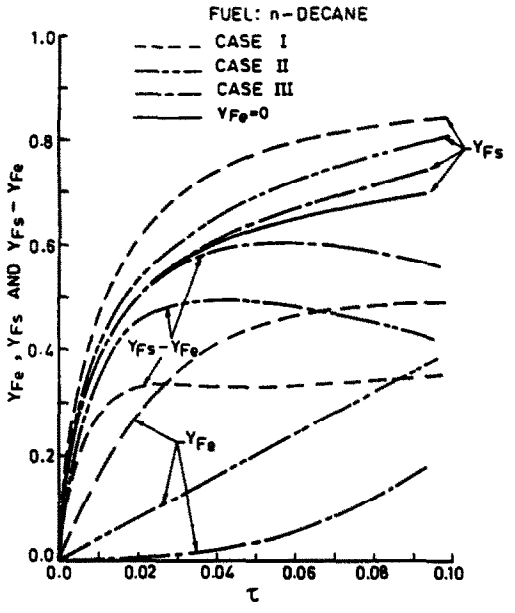

FIG. 7. Temporal variation of surface fuel mass fraction, ambient fuel mass fraction and $(Y_{F_s}-Y_{F_e})$.

droplet surface temperatures well below the saturation temperature.

Similar observations are made for n-hexane and n-hexadecane droplets. In the case of n-hexane droplets the lifetime is not affected much because of the smaller heat-up period due to its higher thermal diffusivity.

Figure 8 shows, for n-decane, the effect of temporal variation of ambient temperature. For case I, the ambient temperature increases from 500 to 1500 K and is lower (compared to $T_e = 1000$ K) during the earlier part of the droplet lifetime. Consequently, the gas-side heat flux, the mass vaporization rate and the liquid-side heat flux will be lower, leading to lower values of surface temperatures during the major part of the droplet lifetime. Consequently, the droplet lifetime is longer. It is also observed that the non-dimensional gas- and liquid-side heat fluxes are higher while the droplet surface temperatures are lower. This is rather misleading unless it is noted that the non-dimensionalizing parameters involve the instantaneous values of ρ_∞, h_∞ and the gas-phase Reynolds number, which vary with the instantaneous temperature. For this reason the actual heat fluxes are lower, even though the non-dimensional heat fluxes are higher.

For case II the ambient temperatures decrease from 1500 to 500 K and are higher compared to 1000 K during the earlier part of the droplet lifetime. It is observed (Fig. 8) that the mass vaporization rate and the heat fluxes are higher (even though the non-dimensional heat fluxes are lower, as explained above) leading to higher surface temperatures during the major part of the droplet lifetime. Consequently, the droplet lifetime is shorter.

From a comparison of these two cases of ambient temperature variations, it can be concluded that the faster rate of droplet heating during the initial part of the droplet lifetime leads to a faster vaporization rate and a shorter lifetime.

Figure 9 shows the effect of ambient pressure variations for n-decane. For case I, the ambient pressure increases linearly from 5 to 15 atm, being lower during the earlier part of the droplet lifetime, compared to the constant value of 10 atm. At lower ambient pressures, the saturation temperatures are lower and consequently the fuel mass fractions are higher, cor-

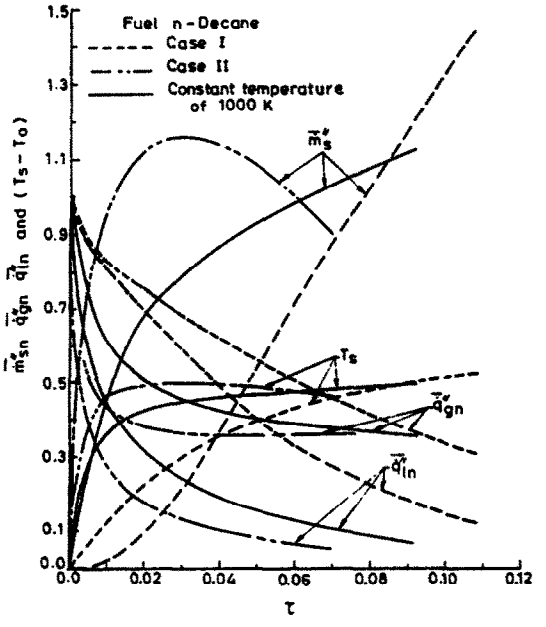

FIG. 8. Effect of temporal variation of ambient temperature.

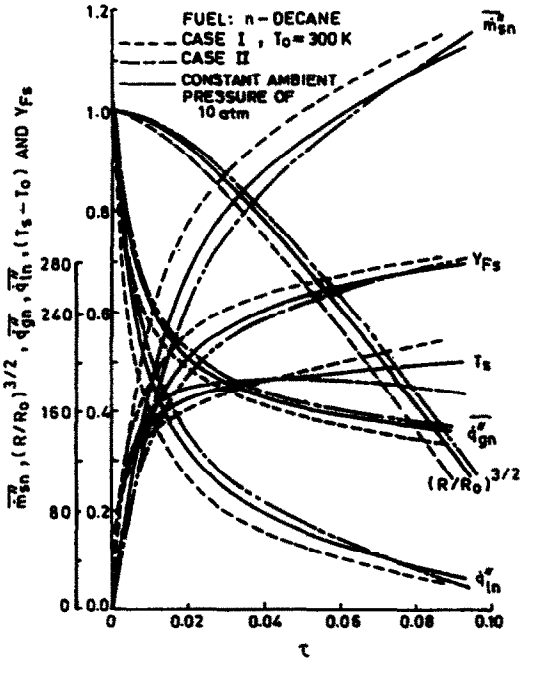

FIG. 9. Effect of temporal variation of ambient pressure.

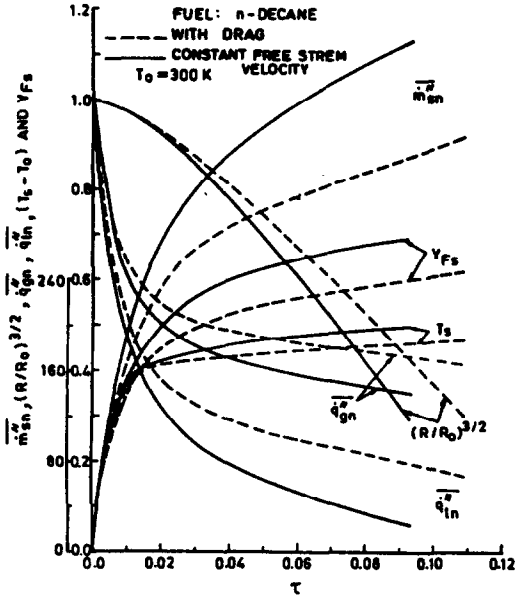

FIG. 10. Effect of drag.

responding to any surface temperature. Therefore, the mass vaporization rate is higher and consequently the droplet lifetime is shorter. It is also observed that during the initial part of the droplet lifetime the surface temperatures are lower while during the latter part they are higher. This is because of the dependence of the heat flux on the ambient pressure, which is more complex. At higher ambient pressures the liquid-side temperature gradients are higher (even though the non-dimensional heat fluxes are lower, because of the higher value of density, ρ_∞, which appears as a non-dimensionalizing parameter), leading to higher droplet surface temperatures.

Similar observations have been made for case II when the ambient pressure decreases linearly from 15 to 5 atm.

Similar conclusions are drawn for n-hexane and n-hexadecane droplets. In the case of n-hexane the droplet lifetime is affected very little. In the situation when the pressure is decreasing, the droplet surface temperature reaches the wet bulb value towards the end of its lifetime and, consequently, the mass vaporization rate increases considerably.

Figure 10 shows, for n-decane, the effect of drag. As expected, it is observed that the mass vaporization rate is lower throughout the droplet lifetime when drag is included. Consequently the droplet lifetime is increased. It is also observed that the non-dimensional heat fluxes are higher when compared with the situation of constant free stream velocity. However, because of the variation in the free stream velocity, U_∞ (which is one of the non-dimensionalizing parameters), the actual heat fluxes are lower, though the non-dimensional fluxes are higher. Consequently, the droplet surface temperature and the mass vaporization rate are lower throughout the droplet lifetime.

CONCLUSIONS

It can be concluded that the integral approach is quite good in predicting the heat and mass fluxes as well as the velocity, temperature and fuel mass fraction profiles across the boundary layer, although the differences are greater for the non-circulating droplet near the point of zero shear stress.

The difference of fuel mass fraction at the droplet surface and in the ambience ($Y_{Fs} - Y_{Fe}$), through its effect on droplet surface temperatures, affects the droplet lifetime, though not significantly.

Also, the rate of droplet heating during the earlier part of the droplet lifetime has a significant effect on the vaporization rate and the droplet lifetime. The higher ambient temperatures during the earlier part of the droplet lifetime significantly enhance the unsteady vaporization rates and consequently reduce the droplet lifetime.

The lower values of ambient pressure, particularly during the earlier part of the droplet lifetime, result in higher vaporization rates mainly because of the higher value of fuel mass fraction. However, the droplet lifetime is not significantly reduced by having lower ambient pressure during the earlier part of its lifetime when compared with a reversed pressure variation.

The mass vaporization rate is reduced and consequently the droplet lifetime is increased because of drag, which results in reduced convective effects.

REFERENCES

1. F. A. Williams, *Combustion Theory* (2nd Edn). Benjamin/Cummings (1984).
2. S. Prakash and W. A. Sirignano, Theory of convective droplet vaporization with unsteady heat transfer in the circulating liquid-phase, *Int. J. Heat Mass Transfer* **23**, 253–268 (1980).
3. S. Prakash and G. Krishan, Convective droplet vaporization with transient non-convective liquid-phase, *Twentieth Symp. (Int.) on Combustion*, pp. 1735–1744 (1984).
4. J. Douglas and B. F. Jones, On predictor–corrector methods for non-linear parabolic differential equations, *J. Soc. Ind. Appl. Math.* **11**, 195–204 (1953).
5. F. H. Garner and R. W. Grafton, Mass transfer in fluid flow from a solid sphere, *Proc. R. Soc. Lond.* **A224**, 64 (1954).
6. M. C Yuen and L. W. Chen, On drag of evaporating liquid droplets, *Combust. Sci. Technol.* **14**, 147–154 (1986).
7. S. A. Morsi and A. J. Alexander, An investigation of particle trajectories in two-phase flow systems, *J. Fluid Mech.* **55**, 193–208 (1972).

VAPORISATION VARIABLE DE GOUTTELETTES DE COMBUSTIBLE DANS UN ENVIRONNEMENT CONVECTIF AVEC DES CONDITIONS D'AMBIANCE VARIABLE

Résumé—On fait une comparaison entre une solution intégrale et celle de la couche limite bidimensionnelle pour la vaporisation variable de gouttelette. Les équations bidimensionnelles quasi-permanentes (découplées de la phase liquide) pour la couche limite de la phase gazeuse axisymétrique sont résolues pour les gouttelettes avec ou sans circulation. L'approche intégrale développée antérieurement (S. Prakash et W. A. Sirignano, *Int. J. Heat Mass Transfer* **23**, 253–268 (1980)) pour l'analyse de la phase gazeuse a été modifiée et étendue aux conditions d'ambiance variable: température, pression, fraction massique de combustible et vitesse d'écoulement libre. On étudie l'effet de la variation de ces paramètres ambiants sur la vaporisation de la gouttelette. On trouve que l'approche intégrale est raisonnablement bonne pour prédire les flux de chaleur et de masse ainsi que les profils de vitesse, de température et de fraction massique de combustible à travers la couche limite. On prédit aussi raisonnablement bien la durée de vie de la gouttelette par l'approche intégrale. La différence de fraction massique entre la surface de la goutte et l'ambiance ($Y_{Fs}-Y_{Fe}$) n'a pas un effet significatif sur la durée de vie. Le flux de chauffage de la goutte pendant la partie initiale de la vie de la goutte a un effet sensible sur la vitesse de vaporisation et la durée de vie. Comme prévu, les taux de vaporisation sont réduits et la durée de vie allongée par la trainée.

INSTATIONÄRE VERDAMPFUNG VON BRENNSTOFFTROPFEN IN EINER KONVEKTIVEN UMGEBUNG UNTER VARIABLEN BEDINGUNGEN

Zusammenfassung—In der vorliegenden Arbeit werden zwei Lösungsmethoden für das Problem der instationären Verdampfung von Tropfen verglichen: eine integrale und eine zweidimensionale Grenzschichtlösung. Die quasi-stationären zweidimensionalen Erhaltungsgleichungen (entkoppelt von der Flüssigphase) für die achsensymmetrische Grenzschicht der Gasphase wurden für zirkulierende und nichtzirkulierende Tropfen gelöst. Ein früher entwickelter Integralansatz (S. Prakash and W. A. Sirignano, *Int. J. Heat Mass Transfer* **23**, 253–268 (1980)) für die Untersuchung in der Gasphase beim Tropfenverdampfungsproblem wurde modifiziert und für zeitabhängige Umgebungsbedingungen erweitert: die Temperatur, den Druck, den Massenanteil des Brennstoffs und die Freistrahlgeschwindigkeit. Die Auswirkungen einer Veränderung dieser Umgebungsparameter auf die Tropfenverdampfung wurde ebenfalls untersucht. Es ergibt sich, daß der Integralansatz die Wärme- und Stoffstromdichten gut vorhersagt, ebenfalls die Profile für Geschwindigkeit, Temperatur und den Massenanteil des Brennstoffs in der Grenzschicht. Auch die Lebensdauer des Tropfens wird befriedigend durch den Integralansatz wiedergegeben. Die Differenz des Brennstoffmassenanteils an der Tropfenoberfläche und in der Umgebung ($Y_{Fs}-Y_{Fe}$) beeinflußt die Oberflächentemperatur und damit die Lebenszeit—wenn auch nicht sehr stark. Die Intensität der Wärmezufuhr an den Tropfen während der frühen Phase seiner Lebensdauer hat einen deutlichen Einfluß auf die Verdampfung und auf die Lebenszeit. Der geringe Umgebungsdruck in der frühen Phase der Lebenszeit bewirkt eine verstärkte Verdampfung. Wie zu erwarten war, wird der Verdampfungsmassenstrom durch den Schlupf verringert, die Lebenszeit des Tropfens erhöht.

НЕСТАЦИОНАРНОЕ ИСПАРЕНИЕ КАПЕЛЬ ТОПЛИВА ПРИ КОНВЕКЦИИ И ИЗМЕНЯЮЩИХСЯ УСЛОВИЯХ ОКРУЖАЮЩЕЙ СРЕДЫ

Аннотация—Сравниваются интегральное и двумерное погранслойное решения задачи нестационарного испарения капель. Квазистационарные двумерные уравнения сохранения (не сопряженные с жидкой фазой) для осесимметричного пограничного слоя в газовой фазе решаются как при наличии, так и отсутствии вращения капель. Интегральный подход, разработанный ранее для анализа области газовой фазы в задаче об испарении капель, модифицирован и расширен для учёта нестационарных условий окружающей среды, а именно, температуры, давления, массовой доли топлива и скорости свободного течения. Исследуется влияние изменения данных параметров окружающей среды на процесс испарения капель. Найдено, что интегральный подход позволяет удовлетворительно определить потоки тепла и массы, а также профили скоростей, температур и массовых долей топлива в пограничном слое. На основе данного подхода также удовлетворительно рассчитывается время жизни капель. Разность массовых долей топлива вблизи поверхности капли и в окружающей среде ($Y_{Fs}-Y_{Fe}$), оказывая влияние на температуру этой поверхности, воздействует, хоть и незначительно, на время жизни капель. Интенсивность нагрева капель в начальный период времени жизни оказывает существенное влияние на скорость парообразования и продолжительность жизни. При низких значениях давления окружающей среды на раннем периоде времени жизни капли процесс парообразования интенсифицируется. Как и ожидалось, при наличии сопротивления массовая скорость парообразования снижается, а время жизни капли возрастает.